JOURNAL OF COMPUTATIONAL PHYSICS 87, 91–107 (1990)

A Numerical Investigation into the Steady Flow Past a Rotating Circular Cylinder at Low and Intermediate Reynolds Numbers

D. B. INGHAM AND T. TANG

Department of Applied Mathematical Studies, University of Leeds, Leeds LS2 9JT, England

Received June 1, 1988; revised March 8, 1989

Numerical solutions have been obtained for steady uniform flow past a rotating circular cylinder. Results are presented for Reynolds numbers, based on the diameter of the cylinder, 5 and 20 and the rotational parameters, α, in the range of $0 \leqslant \alpha \leqslant 3$. To avoid the difficulties in satisfying the boundary conditions at large distances from the cylinder a new numerical technique is introduced. Further, series expansion solutions are obtained which are valid at small values of α, but the results are found to be applicable over a wide range of values of α. The calculated values of the drag and lift coefficients and the general nature of the streamline patterns are in good agreement with the most recent time-dependent calculations performed by Badr and Dennis.

1. INTRODUCTION

Fluid flow past a circular cylinder which is in steady motion, or has been started from rest, in a viscous fluid has long been of interest both experimentally and theoretically (see, e.g., [1–8]). In the present work we shall consider the asymmetrical flow of a viscous fluid which is generated by rotating a circular cylinder in a uniform stream of fluid. There are two basic parameters in the problem, namley, the Reynolds number, defined as $\mathrm{Re} = 2aU/\upsilon$ where υ is the coefficient of kinematic viscosity of the fluid, U the unperturbated main stream speed (in the positive x direction), a the radius of the cylinder, and the rotational parameter $\alpha = a\omega_0/U$, which is a dimensionless measure of the speed of rotation, where ω_0 is the angular velocity of the rotating cylinder. When $\alpha = 0$ the motion is symmetrical about the direction of translation and this situation has previously received a considerable amount of attention, e.g., Dennis and Chang [9] and Fornberg [6, 7] who both provide a comprehensive list of references. The problem of the flow past a rotating cylinder is of fundamental interest for several reasons, e.g., in boundary layer control on aerofoils [10] and the lift force experienced by the cylinder is an example of the Magnus effect and this has been used for lift enhancement [11].

Although there are numerous computations in existence of two-dimensional symmetrical flows, both steady and unsteady, about various shapes of cylinders in

0021-9991/90 $3.00

an unbounded fluid, very little theoretical and numerical work has been reported on either the steady or unsteady flow past a rotating circular cylinder. The earliest numerical solutions of the Navier–Stokes equations at non-zero values of α were given by Thoman and Szewczyk [12]. They obtained numerical results for Reynolds numbers $1 \leqslant \mathrm{Re} \leqslant 10^6$ and rotational parameters $0 \leqslant \alpha \leqslant 6$ and they compared their results with the experimental results of Swanson [13] and Prandtl and Tietjens [14]. Lyul'ka [15] studied the problem for Reynolds numbers, $\mathrm{Re} = 0$, 2, 10, 15, 20, and the values of the rotational parameter in the range of $0 \leqslant \alpha \leqslant 5$. The problem was formulated in terms of the stream function ψ and the vorticity ω and the time dependent form of the governing equations were solved until the steady-state solution was obtained. Badr and Dennis [16] examined the boundary layer growth over the cylinder surface and the formation of the non-symmetrical wake at the rear of the cylinder by considering the time-dependent viscous flow past a rotating circular cylinder. In their numerical method the stream function ψ and vorticity ω were expressed in terms of a complete Fourier series with coefficients depending on space and time and the variations with time of C_L and C_D were obtained.

There has only been a few numerical calculations performed for the case of steady flow past a rotating circular cylinder by employing the steady-state Navier–Stokes equations. Ta Phuoc Loc [17] obtained results for $\mathrm{Re} = 5$ and 20 by solving the Navier–Stokes equations numerically within a finite region surrounding the cylinder subject to a boundary condition on the perimeter of the domain which he states is consistent with the external flow. However, it is found that even in the symmetrical flow situation his results for the drag coefficient are substantially higher than the recent, and most accurate, results obtained by Fornberg [6, 7]. This may be due to the use of a computational region which is too small and the form of the approximation of his outer boundary condition. Ingham [18] reconsidered the numerical solution for the same parameters as investigated by Ta Phuoc Loc using several "possible" boundary conditions at a finite but sufficiently large distance from the cylinder. The calculated stream patterns were similar to those of Ta Phouc Loc but there were considerable discrepancies in the lift and drag coefficients between the results. Moreover, Ingham's lift coefficients C_L vary considerably with the form of external boundary condition assumed, particularly for $\alpha = 0.5$. This effect is also present in the drag coefficient C_D albeit to a lesser effect. It should be pointed out here that the sign of equation (17) of Ingham's paper (p. 354) is in error and this should read, $C_{LF} = (2/\mathrm{Re}) \int_0^{2\pi} (\zeta)_{\xi=1} \cos\theta \, d\theta$. Thus the results presented by Ingham will be inaccurate and all of the signs for his values of C_{LF} are corrected in this paper.

Although there is some agreement amongst these numerical results, they are not entirely consistent in their conclusions. For example, the investigators of [15–18] predict that C_L is in direct proportion with α for $\mathrm{Re} = 20$ and small values of α but the constants of proportionality show considerable discrepancies. Also at this Reynolds number the numerical results of [15, 18] suggest that C_D increases as α increases but this was disputed by [16, 17]. Since there exists a substantial dif-

ference in many properties in the published results and the reasons for this have not been fully understood, even for small values of α, the problem requires considerable further attention.

Analytically, Glauert [19, 20] considered the steady flow for high Re and both large and small values of α on the basis of boundary-layer theory and was able to correlate the circulation round a countour at the edge of the boundary-layer with α. Wood [21] and Moore [3] obtained results generally consistent with those of Glauert from their steady-state theoretical work. It was shown by Moore [3] that the effect of the uniform stream can be regarded as a small perturbation of the rotational flow due to the cylinder, and that a uniformly valid first approximation to the flow fluid can be obtained in this way. Moreover, a uniformly valid second approximation to the velocity distribution was found when $\mathrm{Re} \geqslant \sqrt{48}$. In all of the investigations it was possible to determine the lift on the cylinder, which was found to increase with α and this is agreement with all the published numerical results.

In obtaining numerical solutions for the problem under investigation here difficulties arise in the determination of the boundary conditions at large distances. This problem has been discussed in detail by several authors (see, e.g., [6, 18, 22]). Even in the symmetrical flow situation Fornberg [6] realised the importance of using the most appropriate form of the boundary condition to be applied at large distances from the circular cylinder. Dennis [22] investigated the steady asymmetrical flow past an elliptical cylinder using the method of series truncation to solve the Navier–Stokes equations with the Oseen approximation throughout the flow. He found that by considering the asymptotic nature of the decay of vorticity at large distances that for asymmetrical flows it is not sufficient merely that the vorticity shall vanish far from the cylinder but it must decay rapidly enough. This problem does not arise in the case of symmetrical flows because the leading term in the asymptotic expansion for the vorticity is identically zero. It is clear that in the case of asymmetrical flows it is more difficult to obtain the most appropriate form of the boundary condition which is to be applied at large distances from the cylinder. Ingham [18] investigated the problem of fluid flow past a rotating circular cylinder using three "possible" boundary conditions and the central difference approximation throughout. The boundary condition which was refered to as problem I is consistent with the work of Fornberg [6] who obtained accurate numerical results in the symmetrical flow. His problem II corresponds to the work of Ta Phuoc Loc [17] and there are many discrepancies between the results of the problems I and II. It is therefore found that although several methods for approximating boundary conditions for steady flow past a rotating cylinder have been proposed, it is not clear which of these approaches is the most appropriate one, especially in view of the results for C_D and C_L obtained.

To avoid the difficulties in satisfying the boundary conditions at large distances from the cylinder a new numerical technique is introduced in this paper. In order to avoid numerical errors introduced by approximating the location of the outer boundary condition exact boundary conditions at infinity are obtained and used in the calculations whereas in most of the previous numerical work the boundary

conditions have been applied at a specific station. The numerical results indicate that the lift coefficient C_L is directly proportional to α for small values of α and therefore a series expansion with respect to α is considered.

2. Basic Equations and the Boundary Conditions

The origin is fixed at the centre of the cylinder and the positive x-axis is in the same direction as that of translation. The steady flow of an incompressible fluid in a fixed two-dimensional Cartesian form can be described by the non-dimensional equations,

$$\frac{\partial(\Psi, \omega)}{\partial(x, y)} + \frac{2}{\mathrm{Re}} \nabla^2 \omega = 0, \tag{2.1}$$

$$\nabla^2 \Psi = -\omega, \tag{2.2}$$

where ω is the scalar vorticity and Ψ is the stream function. It is required to solve Eqs. (2.1) and (2.2) subject to the boundary conditions

$$\Psi = 0, \qquad \frac{\partial \Psi}{\partial r} = -\alpha, \qquad \text{on} \quad r = 1, \quad 0 \leqslant \theta < 2\pi, \tag{2.3}$$

$$\frac{\partial \Psi}{\partial r} \to \sin\theta, \qquad \frac{1}{r}\frac{\partial \Psi}{\partial \theta} \to \cos\theta, \qquad \text{as} \quad r \to \infty, \quad 0 \leqslant \theta < 2\pi, \tag{2.4}$$

where (r, θ) are the polar coordinates which are chosen such that $\theta = 0$ coincides with the positive x-axis. For the convenience of numerical computation, we introduce the perturbation stream function ψ, $\psi = \Psi - y$.

Filon [23] showed that the asmptotic form for the stream function at large distances from the cylinder and outside the wake region is

$$\psi \sim \frac{C_L \ln r}{2\pi} + \frac{C_D}{2\pi}(\theta - \pi), \qquad \omega \sim 0, \quad r \to \infty, \quad 0 \leqslant \theta < 2\pi. \tag{2.5}$$

Since the stream function and vorticity equations are both elliptical in nature we should supply one condition for each of the variables at infinity rather than use directly conditions (2.3) and (2.4). It was found that the choice of the boundary condition for the vorticity ω is not as sensitive as that for the stream function ψ (see, [6, 7, and 18]). Hence many authors have paid particular attention to boundary conditions for ψ at large distances from the cylinder. The question of the most appropriate boundary condition for ψ is very involved. Actual physical information has to be supplied through the outer boundary and it will propagate immediately to the interior. The use of a large distance $r = r_\infty$, at which the outer boundary condition is enforced together with inappropriate boundary values does not give

reasonable accuracy, even in the case of $\alpha = 0$ and small values of Re. Usually authors have used one of four possible boundary conditions for ψ, namely

(a) *The Oseen approximation.* Dennis [22] investigated the steady asymmetrical flow past an elliptical cylinder by solving the Navier–Stokes equations with this method. However, even in the symmetrical flow situation Fornberg [6] showed that this boundary condition can be expected to be accurate at most at very small values of the Reynolds number. He plotted ψ and ω as a function of r_∞ and displayed the maximum vorticity on the body surface also as a function of r_∞. The results indicated quite significant errors even for Reynolds numbers as small as 2.

(b) *Ta's method.* When solving the problem as investigated in this paper Ta Phuoc Loc used the boundary condition

$$\psi = -\frac{\sin\theta}{r_\infty} + \alpha \ln(r_\infty), \qquad \text{at} \quad r = r_\infty, \quad 0 \leqslant \theta < 2\pi. \tag{2.6}$$

This expression being the sum of the potential solution for the uniform flow past the circular cylinder with no rotation and the viscous solution for the rotation of the circular cylinder with no uniform flow. There appears to be no rigorous mathematical justification of condition (2.6) and hence the numerical results with this boundary condition cannot be expected to be accurate. In fact, it was seen that even in the symmetrical flow situation Ta's results for C_D are about 10% too high.

(c) *First term approximation.* In the symmetrical situation it is known that outside the wake region that the value of ψ for large values of r will tend to a linear function in θ and that ψ satisfies a Laplace's equation in r and θ. The use of the free stream, i.e., imposing $\psi = 0$ at some finite values r_∞, is very crude and simple. Nevertheless, this has been used in many previous studies even when r_∞ has been taken relatively small (see, e.g., [24–31]). However, Fornberg [6] concluded from his calculations that very large errors are introduced by using this approximation. In the case of asymmetrical flow, Ingham [18] used this condition in order to study the accuracy and came to a similar conclusion as that reached by Fornberg. In particular, the results of C_L given by this method appeared very inaccurate.

(d) *Normal derivative constant.* If we use an exponential scaling in the radial direction, i.e., $r = e^\xi$, from (2.5) we have, outside the wake region,

$$\psi \sim \frac{C_L \xi}{2\pi} + \frac{C_D}{2\pi}(\theta - \pi), \qquad 0 < \theta < 2\pi, \quad \xi \to \infty, \tag{2.7}$$

which yields that

$$\frac{\partial \psi}{\partial \xi} \sim \frac{C_L}{2\pi}, \qquad 0 < \theta < 2\pi, \quad \xi \to \infty. \tag{2.8}$$

In the symmetrical flow situation, we have $C_L = 0$ and Fornberg investigated the condition of "normal derivative zero," i.e., $\partial\psi/\partial\xi = 0$. This condition is easy to

supply (for instance, it requires no evaluation of C_D which is required for the Oseen approximation). Fornberg showed that on implementing this condition he could obtain accurate solutions for Reynolds numbers up to about 40. Thus, Ingham employed the "normal derivative constant" approximation, i.e., $\partial\psi/\partial\xi = C_L/2\pi$. This method uses more terms in the asymptotic expansion for ψ at large values of r_∞ than those of (b) and (c), as discussed above, and one may expect that the results obtained are more accurate. However, it remains to be seen if yet more terms are required in order to obtain very accurate solutions.

(e) *Exact boundary condition.* Because of the importance of the choice in using the most appropriate boundary condition for ψ at large distances from the cylinder we now investigate a method which avoids making this decision. We note from the asymptotic expression (2.5) that

$$\psi/r \to 0 \qquad \text{as} \quad r \to \infty. \tag{2.9}$$

Hence we introduce the transformations

$$\xi = 1/r, \qquad \eta = 2\theta/\pi, \tag{2.10}$$

and

$$f(r, \theta) = \psi(r, \theta)/r; \qquad \text{i.e.,} \quad f(\xi, \eta) = \xi\psi(\xi, \eta). \tag{2.11}$$

Thus we have $f \equiv 0$ on $\xi = 0$ (i.e., $r = \infty$) and this requires no approximation for ψ on the outer boundary.

With transformation (2.10), the flow region $(1 \leqslant r < \infty,\ 0 \leqslant \theta < 2\pi)$ is transformed into a finite rectangular region of the (ξ, η) plane $(0 \leqslant \xi \leqslant 1,\ 0 \leqslant \eta < 4)$. Substituting from (2.10) and (2.11) in (2.1) and (2.2), we obtain

$$-\frac{2\xi^2}{\pi}\frac{\partial(f, \omega)}{\partial(\xi, \eta)} + \frac{2\xi}{\pi} f \frac{\partial\omega}{\partial\eta} + \xi^2 \frac{\partial\omega}{\partial\xi}\cos(\pi\eta/2) + \frac{2\xi}{\pi}\frac{\partial\omega}{\partial\eta}\sin(\pi\eta/2)$$
$$+ \frac{2}{\mathrm{Re}}\left[\xi^4 \frac{\partial^2\omega}{\partial\xi^2} + \frac{4\xi^2}{\pi^2}\frac{\partial^2\omega}{\partial\eta^2} + \xi^3\frac{\partial\omega}{\partial\xi}\right] = 0, \tag{2.12}$$

$$\xi^3 \frac{\partial^2 f}{\partial\xi^2} + \frac{4\xi}{\pi^2}\frac{\partial^2 f}{\partial\eta^2} - \xi^2\frac{\partial f}{\partial\xi} + \xi f = -\omega, \tag{2.13}$$

with $0 \leqslant \xi \leqslant 1$, $0 \leqslant \eta < 4$. The boundary conditions (2.3) and (2.4) become

$$f = -\sin(\pi\eta/2), \qquad \partial f/\partial\xi = \alpha, \qquad \text{on} \quad \xi = 1, \quad 0 \leqslant \eta < 4, \tag{2.14}$$

$$f = 0, \qquad \omega = 0, \qquad \text{on} \quad \xi = 0, \quad 0 \leqslant \eta < 4, \tag{2.15}$$

and since the solution is periodic we also require that

$$f(\xi, 4) = f(\xi, 0), \qquad \omega(\xi, 4) = \omega(\xi, 0), \qquad 0 \leqslant \xi \leqslant 1. \tag{2.16}$$

3. Numerical Method

In order to obtain numerical solutions of Eqs. (2.12)–(2.16), the region of integration $0 \leqslant \xi \leqslant 1$, $0 \leqslant \eta < 4$ is covered by a square mesh of size h and central finite difference approximations to the differential equations (2.12) and (2.13) are employed. In practice, a mesh system is set up such that the mesh size in both ξ and η directions is $h = 1/N$, where N is a predescribed positive integer. In view of the periodic conditions (2.16), an extra line of computation $\eta = 4 + h$ for $0 \leqslant \xi \leqslant 1$ is introduced. Then we have $(N+1) \times (M+1)$ mesh points, where $M = 4N + 1$. The mesh points (ξ_i, η_j) $(0 \leqslant i \leqslant N,\ 0 \leqslant j \leqslant M)$ are (ih, jh). If subscripts 0, 1, 2, 3, and 4 denote quantities at the grid points (ξ_0, η_0), $(\xi_0, \eta_0 - h)$, $(\xi_0 + h, \eta_0)$, $(\xi_0, \eta_0 + h)$, and $(\xi_0 - h, \eta_0)$, respectively, then Eqs. (2.12) and (2.13) may be written in finite difference form, using central differences throughout, as

$$\left(\frac{1}{2} + \frac{2}{\pi^2 \xi_0^2} - \frac{h^2}{4\xi_0^2}\right) f_0 = \frac{1}{\pi^2 \xi_0^2} f_1 + \left(\frac{1}{4} - \frac{h}{8\xi_0}\right) f_2 + \frac{1}{\pi^2 \xi_0^2} f_3 + \left(\frac{1}{4} + \frac{h}{8\xi_0}\right) f_4 + \frac{h^2}{4\xi_0^3} \omega_0, \tag{3.1}$$

$$\left(\frac{1}{2} + \frac{2}{\pi^2 \xi_0^2}\right) \omega_0 = \left(\frac{1}{\pi^2 \xi_0^2} - a(\xi_0, \eta_0)\right) \omega_1 + \left(\frac{1}{4} + b(\xi_0, \eta_0)\right) \omega_2 + \left(\frac{1}{\pi^2 \xi_0^2} + a(\xi_0, \eta_0)\right) \omega_3 + \left(\frac{1}{4} - b(\xi_0, \eta_0)\right) \omega_4, \tag{3.2a}$$

with

$$a(\xi_0, \eta_0) = \operatorname{Re} v_0 h/(8\pi\xi_0^2) + \operatorname{Re} h(f_0 + \sin(\pi\eta_0/2))/(8\pi\xi_0^3), \tag{3.2b}$$

$$b(\xi_0, \eta_0) = h/(8\xi_0) + \operatorname{Re} u_0 h/(8\pi\xi_0^2) + \operatorname{Re} h \cos(\pi\eta_0/2)/(16\xi_0^2), \tag{3.2c}$$

where (u_0, v_0) are defined as

$$u_0 = \frac{\partial f}{\partial \eta}(\xi_0, \eta_0), \qquad v_0 = -\frac{\partial f}{\partial \xi}(\xi_0, \eta_0). \tag{3.3}$$

We now briefly outline how the boundary conditions (2.14)–(2.16) can be implemented:

Boundary conditions for ω

$$\text{On} \quad \xi = 0, \quad 0 \leqslant \eta \leqslant 4: i = 0, \quad 0 \leqslant j < M; \qquad \omega_{0j} = 0. \tag{3.4}$$

On $\xi = 1$, $0 \leqslant \eta < 4$: $i = N$, $0 \leqslant j < M$; in this case we use (2.14) to obtain the vorticity using the second-order accurate finite difference approximation

$$\omega_{Nj}=\left[f_{Nj}-f_{N-1j}-\alpha\left(h-\frac{1}{2}h^2\right)-\frac{1}{6}h^2\omega_{N-1j}\right]\Big/\left[\frac{h^2}{3}(1+h)\right]. \tag{3.5}$$

On $\eta=4+h$, $0\leqslant\xi\leqslant 1: 0\leqslant i\leqslant N$, $j=M$; $\omega_{iM}=\omega_{i1}$. (3.6)

On $\eta=0$, $0\leqslant\xi\leqslant 1: 0\leqslant i\leqslant N$, $j=0$; $\omega_{i0}=\omega_{iM-1}$. (3.7)

Boundary conditions for f

On $\xi=0$, $0\leqslant\eta\leqslant 4: i=0$, $0\leqslant j<M$; $f_{0j}=0$; (3.8)

On $\xi=1$, $0\leqslant\eta\leqslant 4: i=N$, $0\leqslant j<M$; $f_{Nj}=-\sin(\pi\eta_j/2)$; (3.9)

On $\eta=4+h$, $0\leqslant\xi\leqslant 1: 0\leqslant i\leqslant N$, $j=M$; $f_{iM}=f_{i1}$; (3.10)

On $\eta=0$, $0\leqslant\xi\leqslant 1: 0\leqslant i\leqslant N$, $j=0$; $f_{i0}=f_{iM-1}$. (3.11)

The resulting finite-difference equation were solved iteratively as described by

defined by

$$C_L=L/2\rho U^2a, \qquad C_D=D/2\rho U^2a, \tag{3.12}$$

and each consists of components due to the friction forces and the pressure. Hence

$$C_L=C_{LF}+C_{LP}, \qquad C_D=C_{DF}+C_{DP}, \tag{3.13}$$

where

$$C_{DF}=-\frac{2}{\mathrm{Re}}\int_0^{2\pi}(\omega)_{\xi=1}\sin\theta\,d\theta, \qquad C_{LF}=-\frac{2}{\mathrm{Re}}\int_0^{2\pi}(\omega)_{\xi=1}\cos\theta\,d\theta, \tag{3.14}$$

$$C_{DP}=-\frac{1}{2}\int_0^{2\pi}(P)_{\xi=1}\cos\theta\,d\theta, \qquad C_{LP}=\frac{1}{2}\int_0^{2\pi}(P)_{\xi=1}\sin\theta\,d\theta, \tag{3.15}$$

where P is the nondimensional pressure on the cylinder. The non-dimensional θ component of the Navier–Stokes equations on the cylinder reduces to

$$\frac{\partial P}{\partial\theta}=-\frac{4}{\mathrm{Re}}\left(\frac{\partial\omega}{\partial\xi}\right)_{\xi=1}. \tag{3.16}$$

The integrals in (3.14) are evaluated directly while those in (3.15) are evaluated by integration by parts. Thus we obtain

$$C_{DP}=-\frac{2}{\mathrm{Re}}\int_0^{2\pi}\left(\frac{\partial\omega}{\partial\xi}\right)_{\xi=1}\sin\theta\,d\theta, \qquad C_{LP}=-\frac{2}{\mathrm{Re}}\int_0^{2\pi}\left(\frac{\partial\omega}{\partial\xi}\right)_{\xi=1}\cos\theta\,d\theta. \tag{3.17}$$

Formulae (3.14) and (3.17) are calculated by means of a second-order accurate finite-difference method and Simpson's rule.

4. Power Series Solution For Small Rotational Parameter ($\alpha \ll 1$)

To solve Eqs. (2.1) and (2.2) we assume expansions for ψ and ω as powers of α in the form

$$\psi = \psi_0 + \alpha\psi_1 + \alpha^2\psi_2 + \cdots, \tag{4.1}$$

$$\omega = \omega_0 + \alpha\omega_1 + \alpha^2\omega_2 + \cdots, \tag{4.2}$$

and using the transformation (2.11), we obtain

$$f = f_0 + \alpha f_1 + \alpha^2 f_2 + \cdots. \tag{4.3}$$

Substituting (4.2) and (4.3) in Eqs. (2.12) and (2.13) and equating coefficients of successive powers of α, we obtain

$$-\frac{2\xi^2}{\pi}\sum_{p=0}^{n}\frac{\partial(f_{n-p},\omega_p)}{\partial(\xi,\eta)}+\frac{2\xi}{\pi}\sum_{p=0}^{n}f_{n-p}\frac{\partial\omega_p}{\partial\eta}+\xi^2\frac{\partial\omega_n}{\partial\xi}\cos\left(\frac{\pi\eta}{2}\right)$$

$$+\frac{2\xi}{\pi}\frac{\partial\omega_n}{\partial\eta}\sin\left(\frac{\pi\eta}{2}\right)+\frac{2}{\mathrm{Re}}\left[\xi^4\frac{\partial^2\omega_n}{\partial\xi^2}+\frac{4\xi^2}{\pi^2}\frac{\partial^2\omega_n}{\partial\eta^2}+\xi^3\frac{\partial\omega_n}{\partial\eta}\right]=0, \tag{4.4}$$

and

$$\xi^3\frac{\partial^2 f_n}{\partial\xi^2}+\frac{4\xi}{\pi^2}\frac{\partial^2 f_n}{\partial\eta^2}-\xi^2\frac{\partial f_n}{\partial\xi}+\xi f_n=-\omega_n, \tag{4.5}$$

with $0\leqslant\xi\leqslant 1$, $0\leqslant\eta\leqslant 4$, and $n\geqslant 0$.

Using boundary conditions (2.14) and (2.15) the functions f_n and ω_n must satisfy

$$f_n=\begin{cases}-\sin(\pi\eta)/2 & \text{if } n=0\\ 0 & \text{if } n\neq 0\end{cases}\quad \text{on } \xi=1,\ 0\leqslant\eta<4, \tag{4.6a}$$

$$\frac{\partial f_n}{\partial\xi}=\begin{cases}1 & \text{if } n=1\\ 0 & \text{if } n\neq 1\end{cases}\quad \text{on } \xi=1,\ 0\leqslant\eta<4, \tag{4.6b}$$

$$f_n=0, \quad \text{on } \xi=0,\ 0\leqslant\eta<4, \tag{4.7a}$$

$$\omega_n=0, \quad \text{on } \xi=0,\ 0\leqslant\eta<4. \tag{4.7b}$$

Substituting (4.2) into (3.14) and (3.17), we obtain

$$C_{DF}=C_{DF}^{(0)}+\alpha C_{DF}^{(1)}+\alpha^2 C_{DF}^{(2)}+\cdots, \qquad C_{LF}=C_{LF}^{(0)}+\alpha C_{LF}^{(1)}+\alpha^2 C_{LF}^{(2)}+\cdots, \tag{4.8}$$

$$C_{DP}=C_{DP}^{(0)}+\alpha C_{DP}^{(1)}+\alpha^2 C_{DP}^{(2)}+\cdots, \qquad C_{LP}=C_{LP}^{(0)}+\alpha C_{LP}^{(1)}+\alpha^2 C_{LP}^{(2)}+\cdots, \tag{4.9}$$

where

$$C_{DF}^{(n)} = -\frac{2}{\mathrm{Re}}\int_0^{2\pi} (\omega_n)_{\xi=1} \sin\theta \, d\theta, \qquad C_{LF}^{(n)} = -\frac{2}{\mathrm{Re}}\int_0^{2\pi} (\omega_n)_{\xi=1} \cos\theta \, d\theta, \tag{4.10}$$

$$C_{DP}^{(n)} = -\frac{2}{\mathrm{Re}}\int_0^{2\pi} \left(\frac{\partial \omega_n}{\partial \xi}\right)_{\xi=1} \sin\theta \, d\theta, \qquad C_{LP}^{(n)} = -\frac{2}{\mathrm{Re}}\int_0^{2\pi} \left(\frac{\partial \omega_n}{\partial \xi}\right)_{\xi=1} \cos\theta \, d\theta, \tag{4.11}$$

with $n = 0, 1, 2, \ldots$.

5. Results

In order to compare the results obtained by the present numerical methods with previously published results we concentrate on values of Reynolds number $\mathrm{Re} = 5$ and 20 and the rotational parameter $\alpha = 0$, 0.1, 0.2, 0.4, 0.5, 1, 2, and 3 and obtain solutions with mesh size $h = \frac{1}{10}, \frac{1}{15}, \frac{1}{20}, \frac{1}{30}$, and $\frac{1}{40}$. All the final results presented in this paper have been obtained using repeated h^2-extrapolation for each value of Re and α.

TABLE I

The Series Expansion Results

	$C_{DP}^{(0)}$	$C_{DF}^{(0)}$	$C_D^{(0)}$	$C_{LP}^{(1)}$	$C_{LF}^{(1)}$	$C_L^{(1)}$	$C_{DP}^{(2)}$	$C_{DF}^{(2)}$	$C_D^{(2)}$
(i)	2.152	1.875	4.027	2.047	0.589	2.636	−0.102	0.013	−0.089
(ii)	2.129	1.860	3.989	1.881	0.434	2.315	−0.010	0.033	0.023
(iii)	2.115	1.845	3.960	2.014	0.499	2.513	−0.062	0.029	−0.033
(iv)	2.109	1.843	3.952	2.091	0.527	2.618	−0.090	0.028	−0.062
(v)	2.107	1.843	3.950	2.132	0.535	2.667	−0.096	0.028	−0.068
(vi)	2.111	1.848	3.959	1.748	0.310	2.058	0.062	0.030	0.092
(vii)	2.097	1.826	3.923	2.185	0.583	2.768	−0.129	0.025	−0.104
(viii)	2.104	1.841	3.945	2.153	0.549	2.702	−0.112	0.026	−0.086
(ix)	2.104	1.843	3.947	2.185	0.545	2.730	−0.104	0.026	−0.078
(x)	2.091	1.815	3.906	2.387	0.709	3.096	−0.218	0.022	−0.196
(xi)	2.106	1.845	3.951	2.145	0.541	2.686	−0.108	0.026	−0.082
(xii)	2.105	1.844	3.949	2.200	0.543	2.743	−0.100	0.026	−0.074
(xiii)	2.107	1.848	3.955	2.121	0.525	2.646	−0.098	0.027	−0.071
(xiv)	2.104	1.843	3.947	2.211	0.544	2.755	−0.098	0.026	−0.072
(xv)	2.104	1.843	3.947	2.222	0.546	2.768	−0.098	0.026	−0.072

Note Values of the lift coefficients C_L and the drag coefficients C_D estimated from various mesh sizes for $\mathrm{Re} = 5$. Rows (i)–(v) give the numerical results for $h = \frac{1}{10}, \frac{1}{15}, \frac{1}{20}, \frac{1}{30}$, and $\frac{1}{40}$, respectively. Rows (vi)–(ix) are the h^2-extrapolated results from (i) and (ii), (ii) and (iii), (iii) and (iv), and (iv) and (v), respectively. Similarly, rows (x)–(xii) are extrapolated from (vi) and (vii), (vii) and (viii), and (viii) and (ix), respectively; rows (xiii)–(xiv) are extrapolated from (x) and (xi), (xi) and (xii), respectively. Row (xv) is the h^2-extrapolation from (xiii) and (xiv).

Most previous investigators have suggested that C_L is directly proportional to α for small values of α although a more detailed comparison of these results shows considerable discrepancies regarding the multiplicative constant. An investigation of Eqs. (4.4) and (4.5) subject to the boundary condition (4.6) and (4.7) gives

$$C_{LF}^{(m)} = C_{LP}^{(m)} = C_L^{(m)} \equiv 0, \qquad \text{for} \quad m \text{ an even positive integer} \tag{5.1a}$$

and

$$C_{DF}^{(m)} = C_{DP}^{(m)} = C_D^{(m)} \equiv 0, \qquad \text{for} \quad m \text{ an odd positive integer.} \tag{5.1b}$$

Tables I and II show the variation of C_{LP}, C_{LF}, C_L, C_{DP}, C_{DF}, and C_D up to second-order terms for $\mathrm{Re} = 5$ and 20, respectively, and they illustrate how the h^2-extrapolation has been performed with the final results that,

$$\left.\begin{aligned} C_{LP} &\sim 2.22\alpha + O(\alpha^3), \\ C_{LF} &\sim 0.55\alpha + O(\alpha^3), \\ C_L &\sim 2.77\alpha + O(\alpha^3); \end{aligned}\right\} \quad \text{for} \quad \mathrm{Re} = 5. \tag{5.2a}$$

$$\left.\begin{aligned} C_{LP} &\sim 2.21\alpha + O(\alpha^3), \\ C_{LF} &\sim 0.33\alpha + O(\alpha^3), \\ C_L &\sim 2.54\alpha + O(\alpha^3); \end{aligned}\right\} \quad \text{for} \quad \mathrm{Re} = 20. \tag{5.2b}$$

TABLE II

The Series Expansion Results

	$C_{DP}^{(0)}$	$C_{DF}^{(0)}$	$C_D^{(0)}$	$C_{LP}^{(1)}$	$C_{LF}^{(1)}$	$C_L^{(1)}$	$C_{DP}^{(2)}$	$C_{DF}^{(2)}$	$C_D^{(2)}$
(i)	1.231	0.802	2.033	1.822	0.303	2.125	0.008	0.023	0.031
(ii)	1.210	0.796	2.006	1.946	0.305	2.251	−0.021	0.027	0.006
(iii)	1.206	0.794	2.000	2.025	0.311	2.336	−0.053	0.027	−0.026
(iv)	1.203	0.794	1.997	2.113	0.322	2.435	−0.093	0.027	−0.066
(v)	1.202	0.794	1.996	2.151	0.326	2.477	−0.110	0.027	−0.083
(vi)	1.193	0.791	1.984	2.045	0.307	2.352	−0.044	0.030	−0.014
(vii)	1.201	0.791	1.992	2.127	0.319	2.446	−0.094	0.027	−0.067
(viii)	1.201	0.794	1.995	2.183	0.331	2.514	−0.125	0.027	−0.098
(ix)	1.201	0.794	1.995	2.200	0.331	2.531	−0.132	0.027	−0.105
(x)	1.204	0.791	1.995	2.164	0.324	2.488	−0.117	0.026	−0.091
(xi)	1.201	0.795	1.996	2.197	0.334	2.531	−0.133	0.027	−0.106
(xii)	1.201	0.794	1.995	2.208	0.331	2.539	−0.135	0.027	−0.108
(xiii)	1.200	0.795	1.995	2.201	0.335	2.536	−0.134	0.027	−0.107
(xiv)	1.201	0.794	1.995	2.209	0.331	2.540	−0.136	0.027	−0.109
(xv)	1.201	0.794	1.995	2.211	0.330	2.541	−0.136	0.027	−0.109

Note. Values of the lift coefficients C_L and the drag coefficients C_D estimated from various mesh sizes for $\mathrm{Re} = 20$ (see Table I).

TABLE III

Variation of C_L and C_D with α for Re = 5 and 20 as Obtained by the Full Navier–Stokes Solution (NS) and the Series Expansion Solution (SE)

	Re = 5				Re = 20			
	C_L		C_D		C_L		C_D	
α	NS	SE	NS	SE	NS	SE	NS	SE
0	0.000	0.000	3.947	3.947	0.000	0.000	1.995	1.995
0.1	0.277	0.277	3.947	3.946	0.254	0.254	1.995	1.994
0.2	0.559	0.554	3.939	3.944	0.514	0.508	1.992	1.991
0.4	1.111	1.107	3.927	3.935	1.024	1.016	1.979	1.978
0.5	1.389	1.384	3.916	3.929	1.283	1.271	1.973	1.959
1	2.838	2.768	3.849	3.875	2.617	2.541	1.925	1.886
2	5.830	5.536	3.506	3.659	5.719	5.082	1.627	1.559
3	9.191	8.304	3.097	3.299	9.074	7.623	1.396	1.014

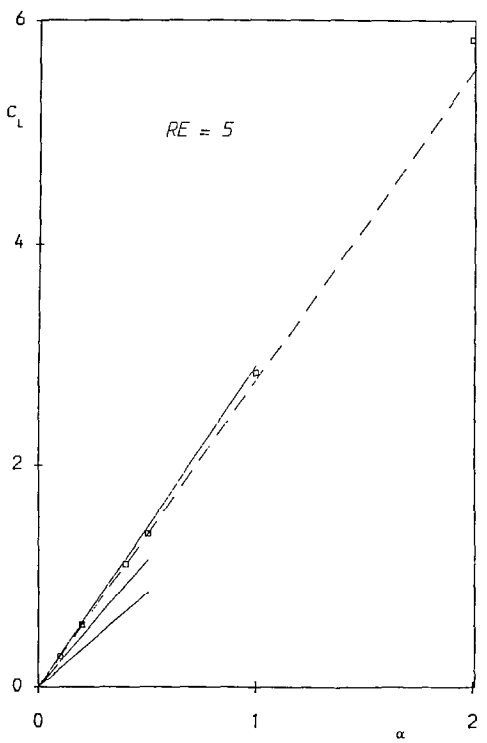

FIG. 1. The variation of C_L with α for Re = 5: □ numerical solutions of the Navier–Stokes equations; – – – series solutions as given in Eq. (5.2); ——— from upper to lower curves the results obtained by Badr and Dennis, Ingham, and Ta Phuoc Loc, respectively.

$$\left.\begin{aligned} C_{DP} &\sim 2.104 - 0.098\alpha^2 + O(\alpha^3), \\ C_{DF} &\sim 1.843 + 0.026\alpha^2 + O(\alpha^3), \\ C_D &\sim 3.947 - 0.072\alpha^2 + O(\alpha^3); \end{aligned}\right\} \quad \text{for} \quad \mathrm{Re} = 5, \tag{5.2c}$$

$$\left.\begin{aligned} C_{DP} &\sim 1.201 - 0.136\alpha^2 + O(\alpha^3), \\ C_{DF} &\sim 0.794 + 0.027\alpha^2 + O(\alpha^3), \\ C_D &\sim 1.995 - 0.109\alpha^2 + O(\alpha^3); \end{aligned}\right\} \quad \text{for} \quad \mathrm{Re} = 20. \tag{5.2d}$$

It is observed that the values of C_D decrease as α increases for both values of Re considered, although the rate of decrease is smaller for $\mathrm{Re} = 5$. This is qualitatively in good agreement with the results of Badr and Dennis [16] and Ta Phuoc Loc [17] but not those of Luyl'ka [15] and Ingham [18]. Further, the accuracy to which the coefficients in the series solution for the drag coefficient have been obtained is much greater than those for the lift coefficient.

In order to check the accuracy of the results presented above, the case of no rotation is compared with the results obtained by previous investigators to this

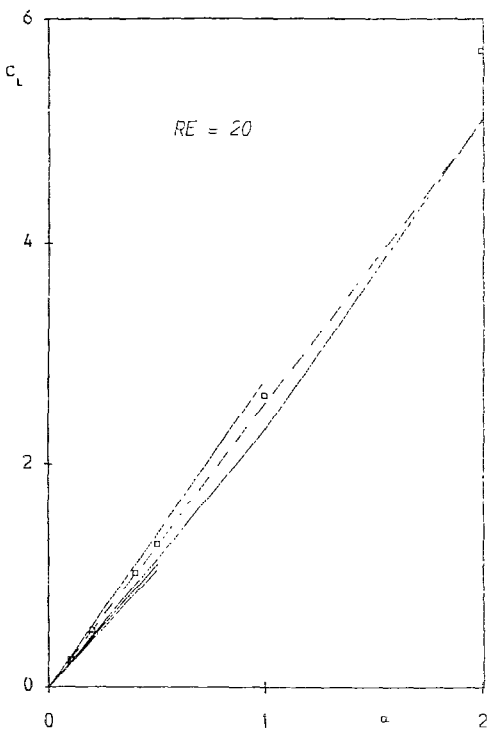

FIG. 2. The variation of C_L with α for $\mathrm{Re} = 20$: □ numerical solutions of the Navier-Stokes equations; – – – series solutions as given in Eq. (5.2); ——— from upper to lower curves the results obained by Badr and Dennis, Lyul'ka, Ingham, and Ta Phuoc Loc, respectively.

problem. The most accurate results of Fornberg [7] suggest that $C_D = 2.0001$ at $\mathrm{Re} = 20$ and this should be compared with the present result of $C_D = 1.995$. However, at $\mathrm{Re} = 5$ we obtain $C_D = 3.947$, $C_{DP} = 2.104$, and $C_{DF} = 1.843$, whereas Dennis and Chang [9] quote values of $C_D = 4.116$, $C_{DP} = 2.119$, and $C_{DF} = 1.917$ which are about 4% higher. It is perhaps relevant to point out that, in the case of intermediate values of the Reynolds number, the drag coefficients estimated by [9] are always a few percent higher than those given by Fornberg [6].

The values of C_D and C_L as obtained by solving the full Navier–Stokes equations are given in Table III for $\mathrm{Re} = 5$ and 20. The values quoted in this table have again been obtained by using repeated h^2-extrapolation and the results are very accurate at small values of α ($\sim 0.1\%$ error) and become less accurate as α increases but are still $O(1\%)$ accurate at $\alpha = 3$. Also shown in Table III are the corresponding values as obtained using the series solution for small values of α as given in Eqs. (5.2). It

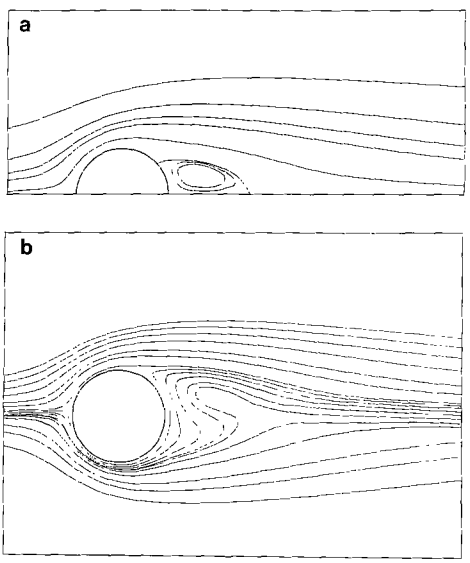

FIG. 3. Streamlines for $\mathrm{Re} = 20$. (a) $\alpha = 0$ (the values of streamlines, starting from the top, are $\psi = 0.5, 0.3, 0.2, 0.1, 0.05$; enclosed streamlines, starting from the centre, are $\psi = -0.004, -0.002, 0$); (b) $\alpha = 0.1$ (the values of streamlines, starting from the top, are $\psi = 0.5, 0.4, 0.3, 0.2, 0.1, 0, -0.01, -0.02, -0.03, -0.04, -0.045, -0.05, -0.06, -0.1, -0.2, -0.3, -0.4, -0.5$); (c) $\alpha = 0.5$ (the values of steamlines, starting from the top, are $\psi = 1, 0.5, 0.3, 0.2, 0.15, 0.1, 0, -0.025, -0.05, -0.1, -0.15, -0.175, -0.2, -0.225, -0.25, -0.3, -0.5, -1$; enclosed streamlines is $\psi = -0.025$); (d) $\alpha = 1$ (the values of streamlines, starting from the top, are $\psi = 0.4, 0.3, 0.2, 0.1\ 0, -0.05, -0.1, -0.175, -0.2, -0.25, -0.3, -0.35, -0.4, -0.425, -0.45, -0.475, -0.5, -0.7, -1$; enclosed streamlines, starting from the inside, are $\psi = -0.05, -0.1$); (e) $\alpha = 2$ (the values of streamlines, starting from the top, are $\psi = 0.5, 0.3, 0.1, 0, -0.1, -0.2, -0.3, -0.4, -0.53, -0.55, -0.6, -0.65, -0.7, -0.75, -0.8, -0.85, -0.9, -1, -1.5, -2, -2.5$; enclosed streamlines, starting from the inside, are $\psi = -0.1, -0.2, -0.3, -0.4, -0.53$); (f) $\alpha = 3$ (the values of streamlines, starting from the top, are $\psi = 0, -0.1, -0.2, -0.3, -0.5, -0.6, -0.8, -1, -1.063, -1.1, -1.15, -1.2, -1.25, -1.3, -1.4, -1.5, -1.75, -2, -2.5, -3$; enclosed streamlines, starting from the inside, are $\psi = -0.1, -0.2, -3, -0.5, -0.6, -0.8, -1$).

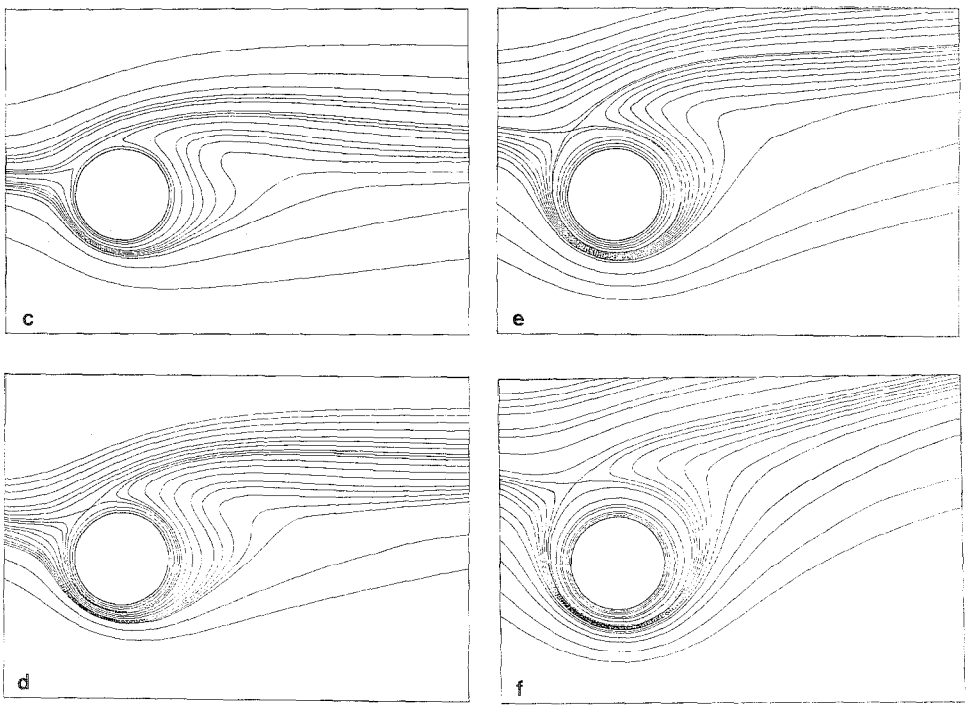

FIG. 3—*Continued*

is observed that the range of validity of the series results given in (5.2) is quite large with results at $\alpha = 0.5$ being at most in error by 1% whilst at $\alpha = 1$ it is 5% in error.

Figures 1 and 2 show the variation of C_L as obtained by solving the full Navier–Stokes equations for $\mathrm{Re} = 5$ and 20, respectively, and $0 \leqslant \alpha \leqslant 2$. Also shown are the series expansion results as given in Eqs. (5.2) and those obtained by [15–18]. The agreement between the full numerical solution and the series solution for $\alpha < 1$ is excellent and there is also reasonable agreement with the results of [16] but the results of [15, 17, 18] severely underestimate the value of the lift coefficient. One of the reasons for this is that most of the previous results have been obtained by using a coarse mesh size.

Despite the many discrepancies between all the previous results in the values of C_L and C_D there is reasonable agreement with other features of the flow, e.g., the surface vorticity and therefore they are not presented in this paper. Figure 3 shows the streamlines for $\mathrm{Re} = 20$ and $\alpha = 0$, 0.1, 0.5, 1, 2, and 3. The streamlines for $\alpha = 0$ can be compared with Dennis and Chang [9] and Fornberg [6] and they are, graphically, indistinguishable. As expected the effect of rotation is to substantially change the streamline pattern near the surface of the cylinder. In the potential flow problem, closed streamlines near the cylinder will only exist if $\alpha > 0.5$, but in the case of viscous flow, closed streamlines will *always* exist for *all* nonzero values of

α. These streamlines only exist very close to the cylinder for small values of α, but as α increases they exist in larger and larger regions as illustrated in Fig. 3. Further, as α increases, an increasing volume of fluid is rotating with the cylinder. For $\mathrm{Re} = 5$ similar streamline patterns exist such as for the case of $\mathrm{Re} = 20$, except that at small values of α where no closed streamlines exist behind the cylinder and hence these results are not presented in this paper. For $\mathrm{Re} = 20$ the effects of rotation annihilate the closed streamline region behind the cylinder and this contrast with the work of Ta Phuoc Loc [17] who finds closed streamlines behind the cylinder for α up to 0.2.

6. Conclusion

In this work we have developed a new numerical technique which avoids the difficulty in satisfying the boundary conditions at large distances from the cylinder. The numerical solutions for the full Navier–Stokes equations have been obtained for $\mathrm{Re} = 5$ and 20 and rotational parameters in the range $0 \leqslant \alpha \leqslant 3$, while the previous investigators present results only for $0 \leqslant \alpha \leqslant 1$. An alternative method of solution, namely, a series expansion method, has also been considered and the resulting finite-difference equations are solved using the new numerical technique. Particular attention has been given to the quantities C_D and C_L since thy are very sensitive to the method of solution. The agreement between the results calculated by the two approaches is very satisfactory over a wide range of values of α.

Acknowledgments

The authors would like to thank Drs. Badr and Dennis for permission to use their unpublished results. One of the authors (T.T.) acknowledges with thanks the University Scholarship provided by the University of Leeds.

References

1. I. Imai, *Proc. Roy. Soc. A* **208**, 487 (1951).
2. M. Kawaguti, *J. Phys. Soc. Japan* **8**, 747 (1953).
3. D. W. Moore, *J. Fluid Mech.* **2**, 541 (1957).
4. F. T. Smith, *J. Fluid Mech.* **92**, 369 (1979).
5. F. T. Smith, *J. Fluid. Mech.* **155**, 175 (1985).
6. B. Fornberg, *J. Fluid. Mech.* **97**, 819 (1980).
7. B. Fornberg, *J. Comput. Phys.* **161**, 297 (1985).
8. H. M. Badr and S. C. R. Dennis, *J. Fluid Mech.* **158**, 447 (1985).
9. S. C. R. Dennis and Gau-Zu Chang, *J. Fluid Mech.* **42**, 471 (1970).
10. J. S. Tennant, W. S. Johnson, and A. Krothapalli, *J. Hydronautics* **10**, 102 (1976).
11. A. T. Sayers, *Int. J. Mech. Elec. Engng.* 7. 75 (1979).
12. D. C. Thoman and A. A. Szewczyk, Tech. Report 66–14, Dept. of Mech. Engng., University of Notre Dame, 1966 (unpublished).

13. W. M. SWANSON, Report, Dept. of Mech. Engng., Case Institute of Technology, 1956 (unpublished).
14. L. PRANDTL AND O. G. TIETJENS, *Applied Hydro and Aeromechanics*, Dover, New York, 1957.
15. V. A. LYUL'KA, *Zh. Vychisl. Mat. Mat. Fiz.* **17**, 470 (1977).
16. H. M. BADR AND S. C. R. DENNIS, private communication, 1986.
17. TA PHOUC LOC, *J. Méc.* **14**, 109 (1975).
18. D. B INGHAM, *Comput. Fluids* **11**, 351 (1983).
19. M. B. GLAUERT, *Proc. Roy. Soc. London A* **230**, 108 (1957).
20. M. B. GLAUERT, *J. Fluid. Mech.* **2**, 89 (1957).
21. W. W. WOOD, *J. Fluid Mech.* **2**, 77 (1957).
22. S. C. R. DENNIS, *Comput. Fluid. Dyn., SIAM-AMS Proc.* **11**, 156 (1978).
23. L. N. G. FILON, *Proc. Roy. Soc. A* **113**, 7 (1926).
24. P. C. JAIN AND M. KAWAKUTI, *J. Phys. Soc. Japan* **21**, 2055 (1966).
25. A. E. HAMIELEC AND J. D. RAAL, *Phys. Fluids* **12**, 11 (1969).
26. P. C. JAIN AND K. SANKARA RAO, *Phys. Fluids Suppl.* II, 57 (1969).
27 R. L. UNDERWOOD, *J. Fluid Mech.* **37**, 95 (1969).
28. F. NIEUWSTADT AND H. B. KELLER, *Comput. Fluids* **1**, 59 (1973).
29. V. A. GUSHCHIN AND V. V. SCHENNIKOV, *Zh. Vychisl. Mat. Mat. Fiz.* **14**, 512 (1974).
30. V. A. PATEL, *Comput. Fluids* **9**, 435 (1981).
31. S.-Y. TUANN AND M. D. OLSON, *Comput. Fluids* **6**, 219 (1978).